

## Study for improvement of grounds subjected to cyclic loads

Satyendra Mittal\* and Kenisevi Meyase

*Department of Civil Engineering, IIT Roorkee - 247667, India*

*(Received July 05, 2011, Revised May 31, 2012, Accepted June 21, 2012)*

**Abstract.** Due to rapid industrialisation, large scale infrastructure development is taking place worldwide. This includes railways, high speed highways, elevated roads etc. To meet the demands of society and industry, many innovative techniques and materials are being developed. In developed nations like USA, Japan etc. for railways applications, new material like geocells, geogrids are being used successfully to enable fast movement of vehicles. The present research work was aimed to develop design methodologies for improvement of grounds subjected to cyclic loads caused by moving vehicles on roads, rail tracks etc. Deformation behavior of ballast under static and cyclic load tests was studied based on square footing test. The paper presents a study of the effect of geo-synthetic reinforcement on the (cumulative) plastic settlement, of point loaded square footing on a thick layer of granular base overlying different compressible bases. The research findings showed that inclusion of geo-synthetics significantly improves the performance of ballasted tracks and reduces the foundation area. If the area is kept same, higher speed trains can be allowed to pass through the same track with insertion of geosynthetics. Similarly, area of machine foundation may also be reduced where geosynthetics is provided in foundation. The model tests results have been validated by numerical modeling, using *FLAC<sup>3D</sup>*.

**Keywords:** ballast; geosynthetics; coefficient of uniform elastic compression; elastic modulus; ground improvement.

---

### 1. Introduction

Due to its economy and ease of construction, reinforced soil has been widely used in geotechnical engineering applications such as the construction of roads, railway embankments, stabilization of slopes, and improvement of soft ground etc. Transportation system such as railway tracks, pavements (highway and airport) and ballasted crane tracks are generally constructed with a layer of granular material within the footing area. The long term satisfactory performance of these structures depends on the repeated loading response of the granular material. Efficacy of granular layer depends on the sub-grade material and its compressibility. Even though the sub-grade may be firm, seasonal softening of a shallow depth from the surface of the sub-grade layer, particularly after heavy rain storms or subgrade thaw, may be sufficient to permit a large settlement failure within the granular material. Loss of granular thickness often results in rutting of the support. Several investigators (Indraratna *et*

---

\*Corresponding author, Ph.D., E-mail: [satyendramittal@gmail.com](mailto:satyendramittal@gmail.com)

*al.* 1998, 2003, Kumar and Awasthi 2008, Kumar and Saxena 2009, Lokesh 2005, Ramesh *et al.* 2010) have studied about improvement of ground subjected to cyclic loads. The present study was aimed at (i) studying the effect of settlement based on static and cyclic load tests (ii) to evaluate the coefficient of elastic uniform compression ( $C_u$ ) by performing laboratory cyclic tests on square footing resting on un-reinforced and reinforced sand beds (iii) investigating the potential use of geogrids for enhancing the performance of soil and ballast (iv) validate the model tests by numerical analysis and (v) suggest the design guidelines.

## 2. Experimental work

### 2.1 Laboratory model tank and the experimental procedures

A rigid steel tank of size  $0.5\text{ m} \times 0.5\text{ m}$  was used as a test set up. The depth of the tank was  $0.4\text{ m}$  (Fig. 1). The wall thickness of tank was  $5\text{ mm}$  and the walls were stiffened by putting cross angle irons. A footing of size  $0.1\text{ m} \times 0.1\text{ m}$  was used for the study. A proving ring of  $5\text{ ton}$  capacity was used for measuring the loading intensity on test footing and two dial gauges were used to record the settlement of footing. A manually operated jack was used to apply loads through proving ring. Static and cyclic load tests were performed in this tank. Flow chart of experimental program is shown in Fig. 2. The ballasts used in tests were sharp, angular aggregates. The soil used in the study was river sand, collected locally from river Solani. The properties of sand and ballast used in the study are given in Table 1. The grain size analysis curves of sand and ballast are given in Figs. 3 and 4 respectively (Mittal and Shukla 2009).

The properties of the different types of Geogrids used in present study are given in the Table 2 and the illustrative representation of geogrids is shown in Fig. 5. The geogrids were selected on the basis of their easy availability and  $D_{50}$  of sand and ballast used in study.

### 2.2 Preparation of test sample

Oven dried sample was used to performed both static and cyclic plate load test. A thick layer of



Fig. 1 Experimental setup of the test

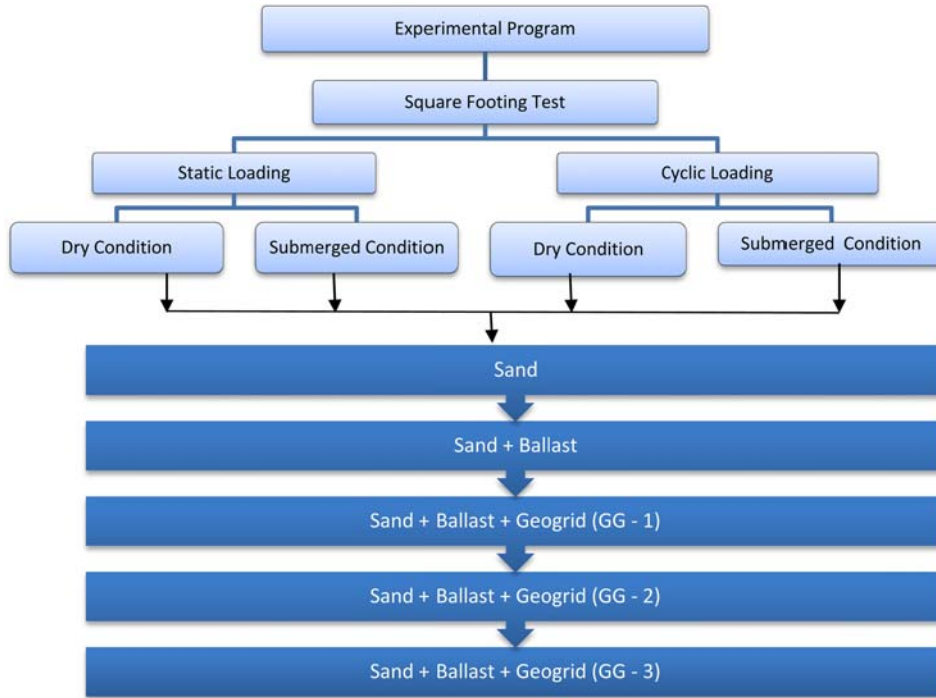


Fig. 2 Flow chart of experimental program

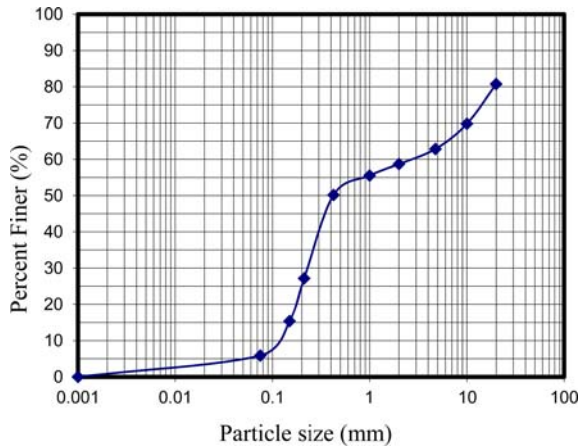


Fig. 3 Grain size analysis curve of sand used in model tests

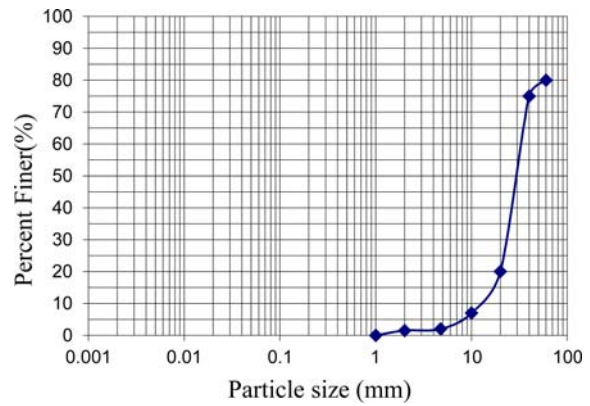


Fig. 4 Grain size analysis curve of sand used in model tests

sand bed of height 0.2 m was poured into the tank and compacted to a density of  $15.3 \text{ kN/m}^3$  to act as leveling pad. Over it another thick layer of ballast was poured of 0.20 m height which was also compacted to maintain a density of  $21 \text{ kN/m}^3$ . Finally a layer of sand in 0.20 m height was poured over the ballast and compacted (Fig. 6). For the reinforced case different geogrids were used and they were placed between sand and ballast layer as shown in Fig. 6(b). A square rigid steel plate ( $200 \text{ mm} \times 200 \text{ mm} \times 25 \text{ mm}$  thick) was used as footing. Two dial gauges were placed on the

Table 1 Basic properties of sand and ballast

Item	Sand	Ballast
Grain specific gravity (Gs)	2.65	2.7
Angle of internal friction ( $\Phi^\circ$ )	32	45
$D_{50}$ (mm)	0.425	30
$C_u$	2	1.2
$C_c$	0.98	1.04
Relative density (%)	35	
$e_{max}$	0.86	
$e_{min}$	0.48	
Unit weight ( $kN/m^3$ )	15.3	21
Soil Classification	SP	GP

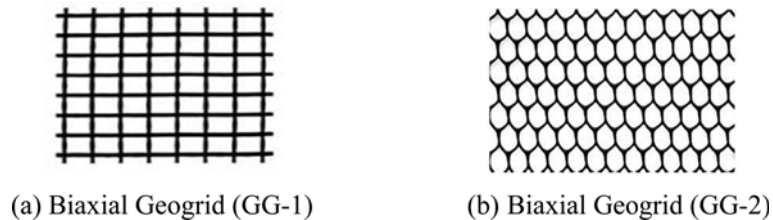


Fig. 5 Different types of Geogrid used in the study

Table 2 Properties of the different geogrids used in the study

Type of geogrid	Aperture size (mm $\times$ mm)	Tensile strength
Biaxial Geogrid (GG-1)	25 $\times$ 25	131 kN/m @20% Strain
Biaxial Geogrid (GG-2)	8 $\times$ 8	121 kN/m @ 20% strain

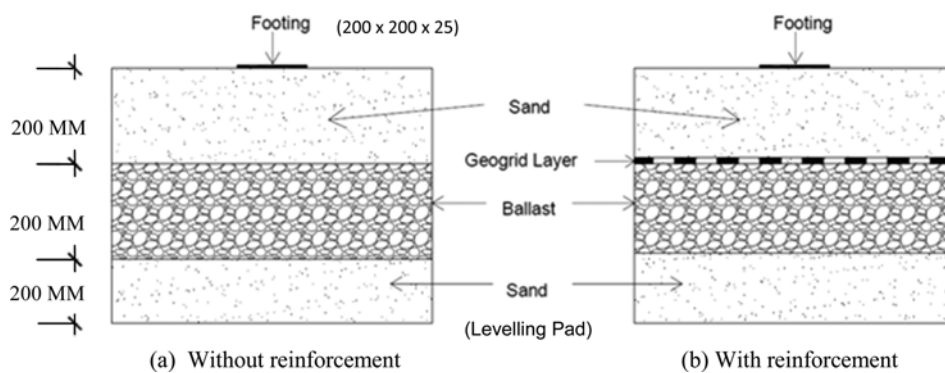


Fig. 6 Cross section of the test specimen

model footing to measure the settlement of footing during loading which was measured through proving ring. In order to provide vertical loading alignment, a small semispherical indentation was

Table 3 Test program

Test series	Type of reinforcement	Aim of tests	No. of tests conducted
Static tests (Dry condition)	Sand, Sand + Ballast, Sand + Ballast + Geogrid (GG-1), Sand + Ballast + Geogrid (GG-2)	Verification of numerical model	4 + 4 = 8
Static tests (Submerged condition)	Sand, Sand + Ballast, Sand + Ballast + Geogrid (GG-1), Sand + Ballast + Geogrid (GG-2)	Verification of numerical model	4 + 4 = 8
Cyclic tests (Dry condition)	Sand, Sand + Ballast, Sand + Ballast + Geogrid (GG-1), Sand + Ballast + Geogrid (GG-2)	Estimation of coefficient of elastic uniform compression ( $C_u$ )	4 + 4 = 8
Cyclic tests (Submerged condition)	Sand, Sand + Ballast, Sand + Ballast + Geogrid (GG-1), Sand + Ballast + Geogrid (GG-2)	Estimation of coefficient of elastic uniform compression ( $C_u$ )	4 + 4 = 8

(Note: For every test, 2 samples were tested under similar conditions to verify the results)

Table 4 Values of friction angle with and without reinforcement

Material	Friction angle ( $\Phi^\circ$ )
Ballast	45
Ballast with Geogrid (GG-1)	51
Ballast with Geogrid (GG-2)	48

made in which a steel ball bearing was placed to apply uniform load on footing without friction at the centre of the footing.

### 2.3 Testing program

Total 32 tests in different series were carried out to study the effect of reinforced soil (with geogrid) and unreinforced soil on the behavior footing. The coefficient of elastic uniform compression of soil ( $C_u$ ) was also computed. The details of test program are listed in Table 3.

### 2.4 Shear test

Direct shear tests were done on ballast with and without geogrids to know the friction angle between the ballast and the geogrid using a large size box 300 mm × 300 mm × 200 mm. The tests were also conducted on triaxial tests on sample sizes of 100 mm × 200 mm. On the basis of these tests, the values of the friction angle for different conditions are tabulated below (Table 4).

## 3. Results and discussions of tests

### 3.1 Static load test

Total 16 static tests were conducted under different conditions. Firstly sand was filled into the

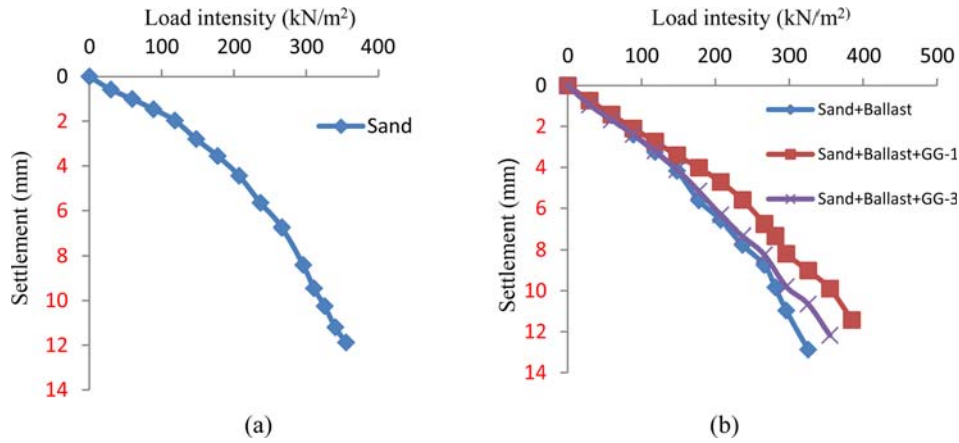


Fig. 7 Variations of applied stress with settlement for different arrangement of sand, ballast and geogrid in dry condition (a) static load on sand and (b) static load on sand + Ballast and with different geogrid

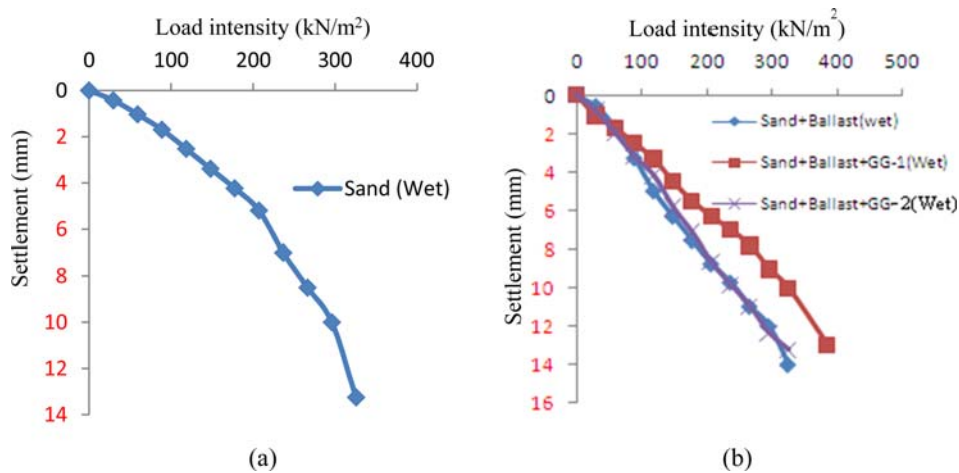


Fig. 8 Variations of applied stress with settlement for different arrangement of sand, ballast and geogrid in saturated condition (a) static load on sand and (b) static load on sand + Ballast and with different geogrids

tank and compacted to the required density to make a leveling pad. After that ballast and sand were used in the test setup described above. Thereafter the tests were performed with different types of geogrid placed between the sand bed and the ballast layer. These tests were conducted both in dry and submerged conditions. Load was applied incrementally with the help of calibrated proving ring. The first load of 29.59 kN/m<sup>2</sup> was applied and the corresponding deflections were noted down with the help of dial gauges provided over the footing. The second load of 59.18 kN/m<sup>2</sup> was applied over the footing and deflections were noted, the process was repeated and each load was applied at an interval of 29.59 kN/m<sup>2</sup>. This was done until the failure of aggregate occurred. The final readings were noted and recorded. Load intensity vs. settlement curves in dry and saturated conditions were plotted. The same are shown in Figs. 7 and 8 respectively. From these figures it was concluded that load carrying capacity was increased when geogrid was placed in between the sand bed and the

Table 5 Comparison of Static Load Intensity in dry and wet condition

Material details	Load intensity (kN/m <sup>2</sup> )	
	Dry	Wet
Sand	150	125
Sand + Ballast	115	90
Sand + Ballast + GG1	147	110
Sand + Ballast + GG2	118	95

ballast. For a settlement of 3 mm (say) the load intensity in dry and wet condition are presented in Table 5.

### 3.2 Cyclic load test

In the cyclic load test, load was applied in a cyclic manner. A load of 29.59 kN/m<sup>2</sup> was applied, dial gauge readings were noted down and load was decreased to zero and again load was increased to 59.18 kN/m<sup>2</sup>. This load was also withdrawn to zero and thus the entire test was done in the above manner till the test specimen failed. This test was also conducted both in wet and dry conditions, with and without geosynthetics as given in Table 3. Load intensity vs. settlement curves in dry conditions are shown in Fig. 9 while load intensity vs. elastic settlement are shown in Fig. 10 and that for submerged conditions, load intensity vs. settlement and load intensity vs. elastic settlement curves are shown in Figs. 11 and 12 respectively. The sequential loading and unloading adopted for all tests made it possible to separate the recoverable component ( $S_e$ ) and non-recoverable component ( $S_p$ ) of the total settlement of the footing for different load levels. The coefficient of elastic uniform compression  $C_u$ , the coefficient of elastic shear  $C_\tau$ , the coefficient of elastic non-uniform shear  $C_\psi$  and the coefficient of elastic non uniform compression  $C_\phi$  are then determined by the relations given below as per IS 5249: 1992.

Table 6 Experimental values of  $C_u$ ,  $C_\tau$ ,  $C_\phi$ ,  $C_\psi$  and  $E$  for unreinforced and various reinforcing conditions of sand beds with geogrid

Material Details	$C_u$ kN/m <sup>3</sup> $\times 10^4$	$C_\tau$ kN/m <sup>3</sup> $\times 10^4$	$C_\phi$ kN/m <sup>3</sup> $\times 10^4$	$C_\psi$ kN/m <sup>3</sup> $\times 10^4$	$E$ kN/m <sup>2</sup> $\times 10^3$
Sand (Dry)	2.08	1.19	4.11	1.79	2.51
Sand + Ballast (Dry)	2.28	1.30	4.50	1.95	2.75
Sand + Ballast + Geogrid (GG-1) (Dry)	3.39	1.94	6.71	2.91	4.10
Sand + Ballast + Geogrid (GG-2) (Dry)	3.16	1.80	6.23	2.7	3.82
Sand + Ballast + Geogrid (GG-3) (Dry)	2.51	1.44	4.97	2.16	3.03
Sand (Wet)	2.01	1.15	3.98	1.72	2.42
Sand + Ballast (Wet)	2.15	1.22	4.25	1.84	2.60
Sand + Ballast + Geogrid (GG-1) (Wet)	3.63	2.08	7.20	3.12	4.38
Sand + Ballast + Geogrid (GG-2) (Wet)	2.88	1.65	5.71	2.48	3.50
Sand + Ballast + Geogrid (GG-3) (Wet)	2.45	1.40	4.84	2.1	2.96

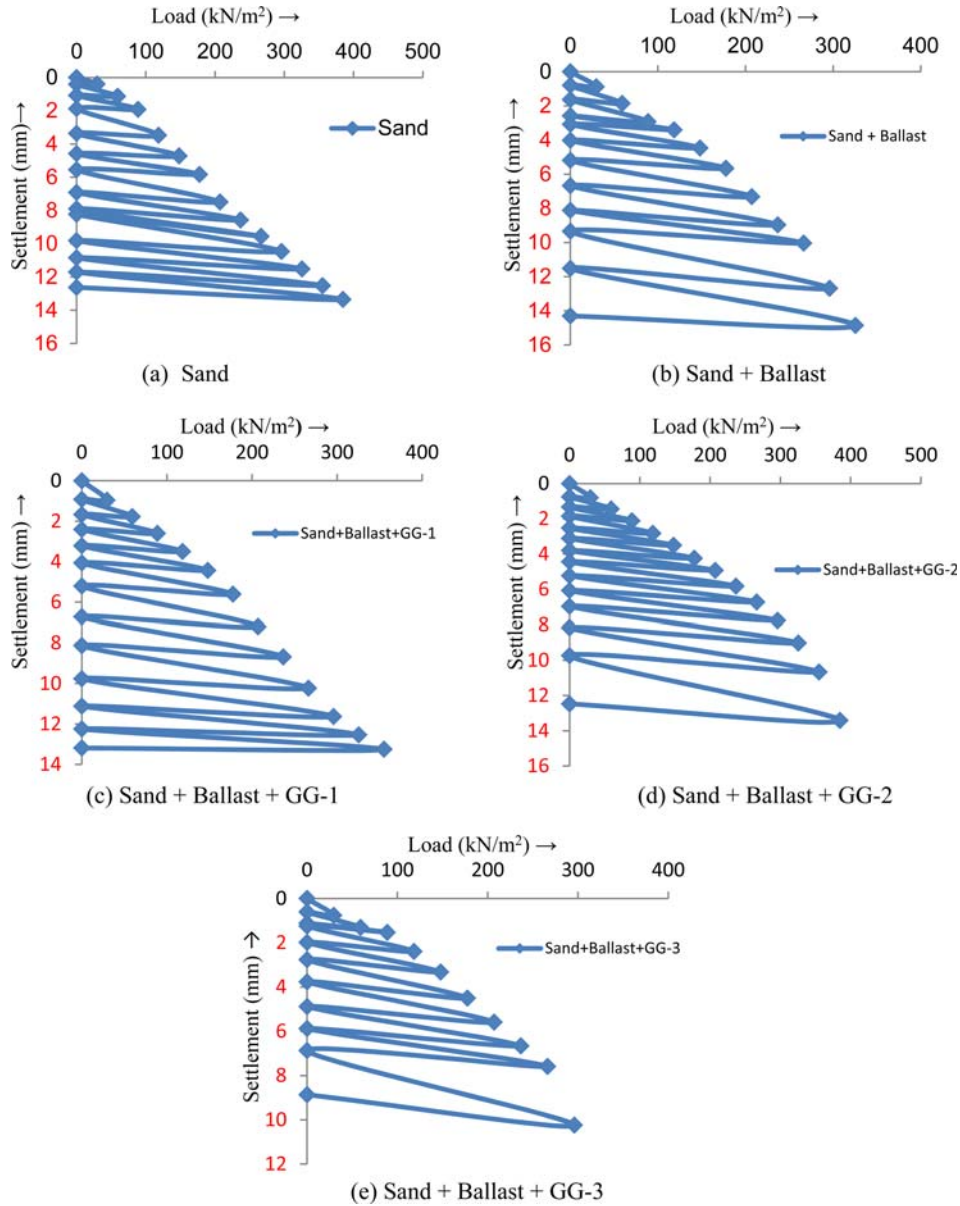


Fig. 9 Variations of applied stress with settlement for different arrangement of sand, ballast and geogrid in dry condition under cyclic loads

$$C_u = p/S_e \text{ kN/m}^3 \tag{1}$$

It can be determined by plotting a graph for  $p$  vs.  $S_e$  as shown in Fig. 10 and Fig. 12.

Where,  $p$  = corresponding load intensity in  $\text{kN/m}^2$  and  $S_e$  = Elastic rebound settlement corresponding to ' $p$ ' in mm.

Barkan (1962) suggested following relationship of  $C_u$  with  $E$  and  $\nu$  as

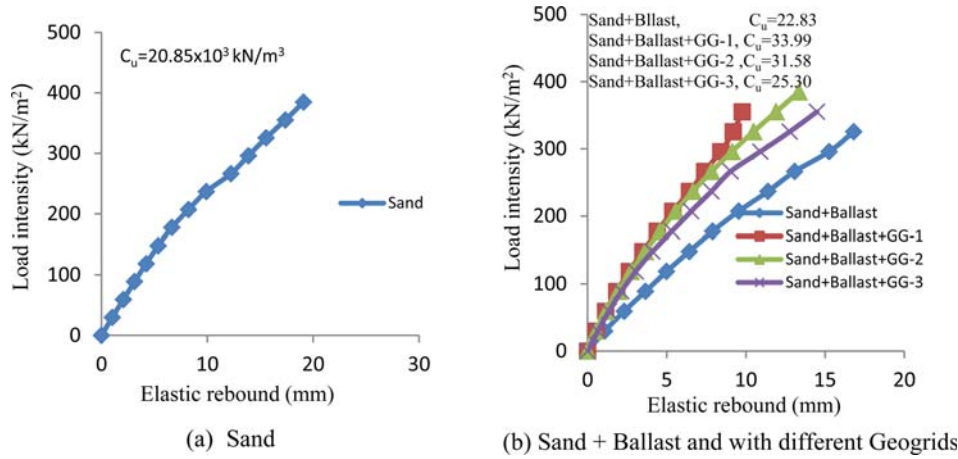


Fig. 10 Variation of Load intensity Vs elastic rebound from cyclic plate load test under dry condition

$$C_u = 1.13 \left( \frac{E}{(1-\nu^2)} \right) \frac{1}{\sqrt{A}} \quad (2)$$

Where,  $E$  = Elastic modulus of soil,  $\nu$  = Poisson’s ratio,  $A$  = Area of base of the foundation

He also developed the relationship between  $C_u$ ,  $C_\phi$ ,  $C_\tau$  and  $C_\psi$  as:

$$C_u = 1.5 \text{ to } 2 C_\tau, C_\phi = 3.46 C_\tau \text{ and } C_\psi = 1.5 C_\tau.$$

The values of the above coefficients and elastic modulus are obtained for different conditions of sand beds and are shown in Table 6. For moving loads like train etc., the subgrade modulus is an important parameter in deciding allowable operational speed of the train (AREA 1996).

#### 4. Numerical analysis

The sand bed, geogrid structural element (geogrid SEL) and the ballast had been modeled using the plastic Mohr-Coulomb model predefined in the  $FLAC^{3D}$  program. The material used in the model could yield and flow. Because of the symmetry of the system, quarter symmetry model had been taken for simulation. A cubical soil grid with appropriate dimensions had been used to construct one fourth of the 3D model. The boundary conditions applied to this domain are sketched in Fig.13.

The model had a dimension of  $0.25 \text{ m} \times 0.25 \text{ m}$  and a depth of  $0.4 \text{ m}$  representing a brick mesh (Fig. 14). Three types of zone models namely brick mesh for bottom sand bed, middle ballast layer and top sand layer had been used for grid generation. The advantage of using the grouping command had been utilized for better grouping of the model such as sand bed, ballast layer and the top sand layer which aid in assigning of material properties.

In  $FLAC^{3D}$  simulation the displacements of the far x-, y- and z-boundaries are restricted in all directions, and the displacements of the symmetry boundaries corresponding to the planes at  $x = 0$  and  $y = 0$  are restricted in the x- and y-directions respectively. The slab is smooth, displacements are free in the x- and y-directions and a velocity is applied in the positive z-direction to grid points

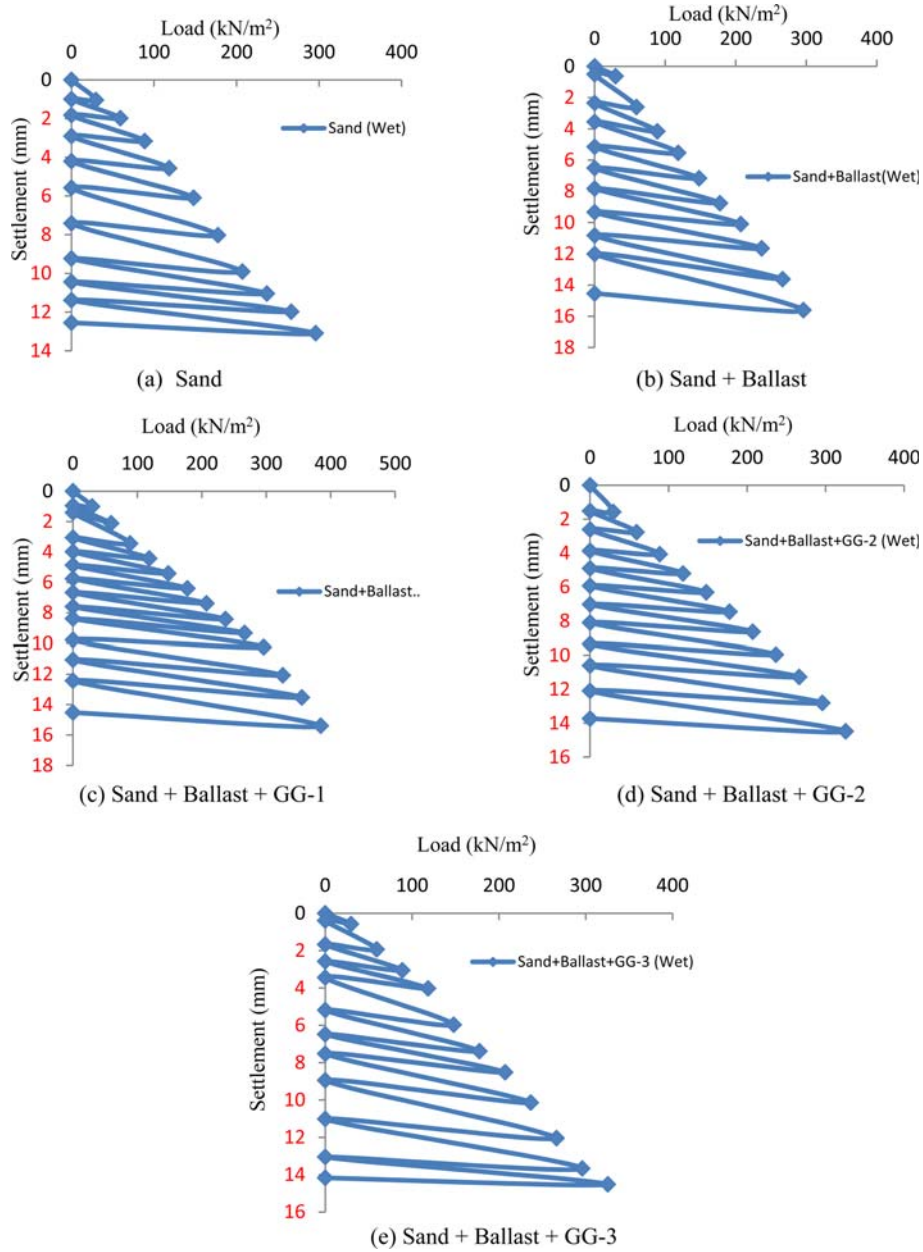


Fig. 11 Variations of applied stress with settlement for different arrangement of sand, ballast and geogrid in wet condition under cyclic loads

within a  $0.25 \text{ m} \times 0.25 \text{ m}$  area to simulate loading of the footing. The domain was discretized into 3500 zones. The area representing the footing covered a total of  $3 \times 3$  zones. For an applied velocity loading, the footing dimensions were,  $a = 0.05 \text{ m}$  and  $b = 0.05 \text{ m}$ . The zone dimensions were graded outside the footing area according to a geometrical progression with factor 1.2 in the x-, y- and z- directions (Fig. 14). A velocity of magnitude  $1.5 \times 10^{-6} \text{ m/step}$  was applied at the nodes within the

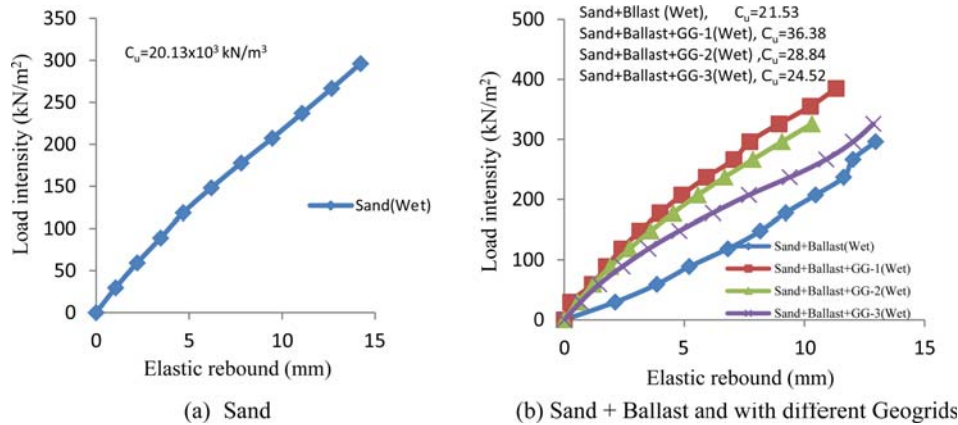


Fig. 12 Variation of Load intensity Vs elastic rebound from cyclic plate load test under wet condition

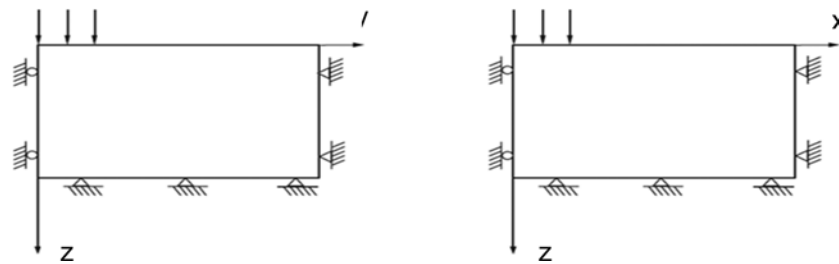


Fig. 13 Boundary conditions for  $FLAC^{3D}$  analysis – quarter symmetry

footing area. The result interpretations were done by plotting load (footing pressure) v/s displacement curve.

#### 4.1 Material properties

The parameters like cohesion, angle of internal friction and Young’s modulus for the numerical simulation were obtained from the large size triaxial tests of specimen size 100 mm × 200 mm. The Young modulus ( $E$ ) was computed from deviator stress v/s axial strain curves obtained from triaxial shear tests, performed at CU conditions. The modulus is defined as slope of initial straight line portion of stress – strain curve. Poisson’s ratio ( $\nu$ ) was also computed on the basis of results of Triaxial tests, where volume change of specimen had been noted during tests with the help of volume change gauge. The Poisson’s ratio was thus computed as –

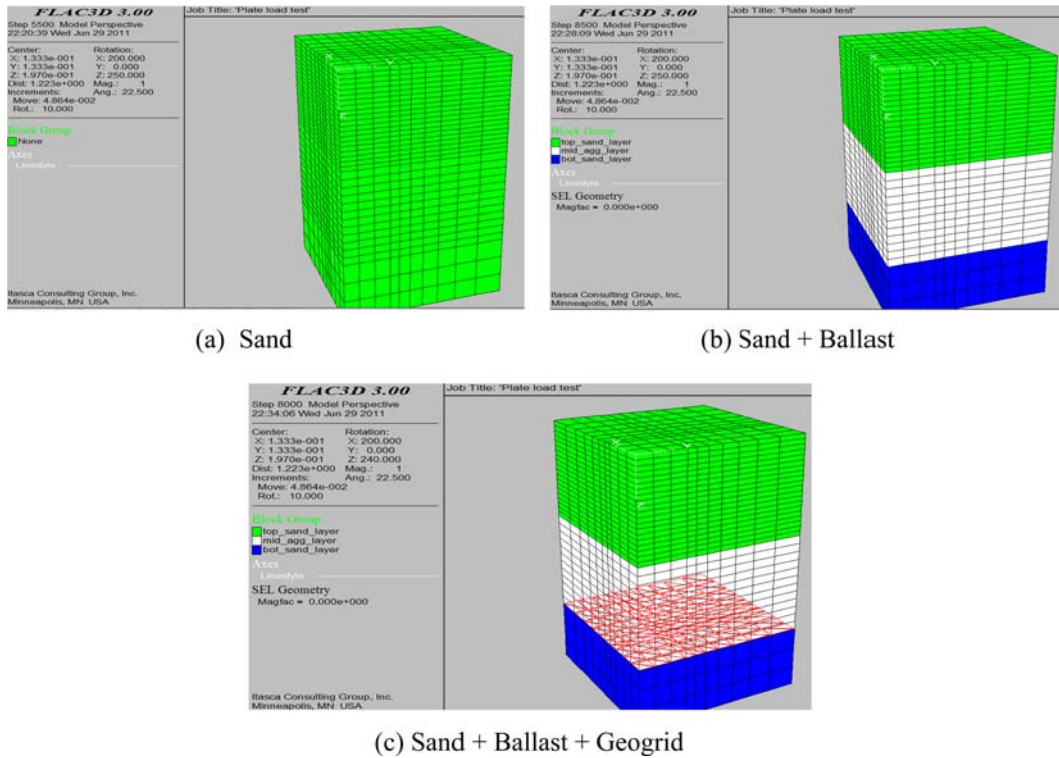
$$\nu = \frac{1}{2} \left[ 1 - \frac{1}{\pi r^2} \left( \frac{\Delta V}{\Delta L} \right) \right] \quad (3)$$

Where  $\Delta V/\Delta L$  is slope of straight line portion of graph between change in volume ( $\text{mm}^3$ ) and change in length (mm). The tests were conducted on 6 samples each for computation of  $E$  and  $\nu$ . The results of all the tests were in close agreement.

Each geogrid SEL possesses the following properties: Isotropic material properties ( $E$  and  $\nu$ ),

Table 7 Material properties used in the numerical model

Material	Shear strength parameters		Young's modulus, $E$ (MPa)	Poisson's ratio, $\nu$	Density, $\gamma_d$ (kN/ m <sup>3</sup> )
	$c$ (kPa)	$\Phi$ (°)			
Sand	0	32	5	0.3	15.3
Ballast	0	45	15	0.33	21



(a) Sand

(b) Sand + Ballast

(c) Sand + Ballast + Geogrid

Fig. 14  $FLAC^{3D}$  grid – quarter symmetry

thickness,  $t$  [L], cs scch as coupling spring cohesion (stress units),  $c$  [ $F/L^2$ ], cs sfrc as coupling spring friction angle,  $\Phi$  [degrees] and cs sk as coupling spring stiffness per unit area,  $k$  [ $F/L^3$ ]. These values are tabulated below (Table 8):

Table 8 Geogrid material properties used in the numerical model

Property	Biaxial geogrid (GG-1)	Biaxial geogrid (GG-2)
Young's modulus, $E$ (GPa)	26	20
Poisson's ratio, $\nu$	0.33	0.3
Thickness (mm)	2	5
cs scch (kPa)	0	0
cs sfrc (°)	25	25
cs sk (N/m <sup>3</sup> )	$2.3 e^6$	$2.2 e^6$

#### 4.2 Numerical study programme

The numerical investigation has been carried out in the sequence as given in the Table 3. The same material properties as tabulated in Tables 5 and 6 had been used in the analysis. A total of 10 different models had been developed depending on dry and wet condition with and without geogrid.

#### 4.3 Verification of numerical model

The accuracy of the used numerical model for static laboratory tests in both dry and wet conditions was verified. To achieve this, ten numbers of numerical analysis on footing under static loading tests were performed, and the results were compared with those of the above-mentioned experiments (Fig. 7 and Fig. 8). The results obtained from tests and numerical analyses had been compared in Fig. 13 and Fig. 14. The results revealed that the maximum difference between test results and numerical analysis was less than 10% and the predictions of numerical analysis were reasonably accurate.

### 5. Analysis of results

After conducting several tests over the ballast, it is concluded that by using the geogrid, the load carrying capacity increases and it improves the settlement behaviour of the ballast significantly. As can be seen from Fig. 7(b), for almost 12 mm settlement the load intensity increases from 300 kN/m<sup>2</sup> for sand + ballast specimen to 384.5 kN/m<sup>2</sup> for sand + ballast + GG-1 specimen. Fig. 8(b) shows that for 13 mm settlement the load intensity increases from 300 kN/m<sup>2</sup> for sand + Ballast specimen to 384.5 kN/m<sup>2</sup> for sand + Ballast + GG-1. The failure load and the corresponding settlement values are tabulated below in Table 9. As can be seen from this table, the settlement value increases for GG-2 as compared to that of GG-1. This may be due to the reason that the tensile strength of GG-1 was more than that of GG-2.

The aim of the present work was also to develop and analyse a suitable *FLAC*<sup>3D</sup> model to simulate the experimental program. The experimental program consisted of static and cyclic loading test. *FLAC*<sup>3D</sup> was used to simulated static load tests only. A total of 10 models had been developed depending upon the requirement of ballast, sand and geogrid. The results obtained have been compared with the experimental findings, and both results are in close agreement (Fig. 15 and Fig. 16).

The experimental results conclude that the load intensity increases with the use of geogrid in between sand and ballast. The numerical analysis too shows the same trend. The settlement also reduces with inclusion of geogrid. The numerical model tests however do not exactly match the experimental results but the percentage difference is between 2 to 10%. Hence though with the limitations in selection of the material properties and the model itself, the numerical model study authenticate the experimental study.

#### 5.1 Application of results of cyclic load tests

By referring Table 5 the coefficient of uniform compression,  $C_u$  for the actual foundation area can be calculated using the following relationship

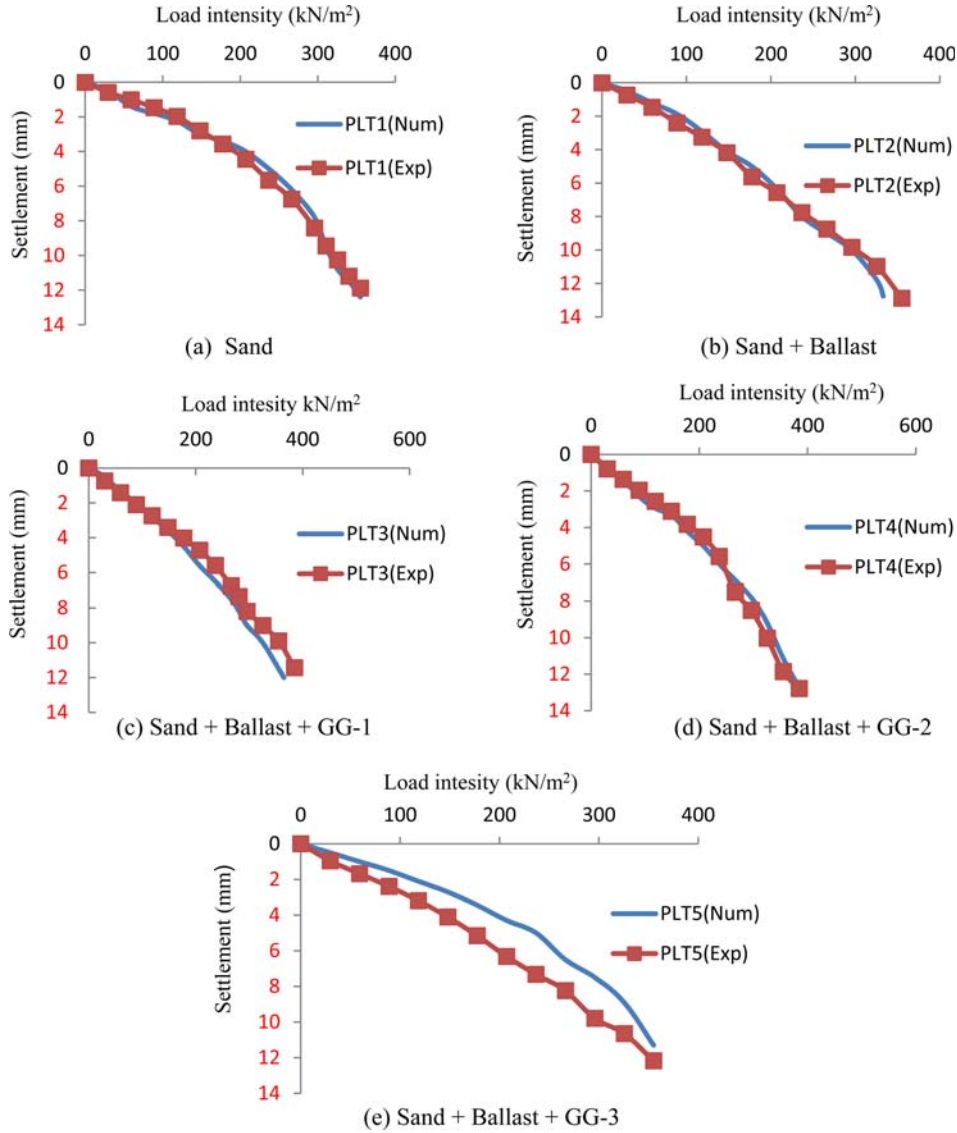


Fig. 15 Validation for square footing of  $150 \times 150$  mm on sand, ballast and different geogrid in box of  $500 \times 500 \times 400$  mm under static load in dry condition

$$C_u \sqrt{A} = C_{u1} \sqrt{A_1} \quad (4)$$

Where  $C_u$  and  $A$  refer to the test plate and  $C_{u1}$  and  $A_1$  to the foundation. The value of  $C_u$  increases with use of geosynthetics, therefore area of foundation shall be automatically reduced.

Also from Eq. (2) as the coefficient of uniform compression ( $C_u$ ) increases, the area of the foundation gets decreased as shown below

$$\sqrt{A} = 1.13 \left( \frac{E}{1 - \nu^2} \right) (1/C_u) \quad (5)$$

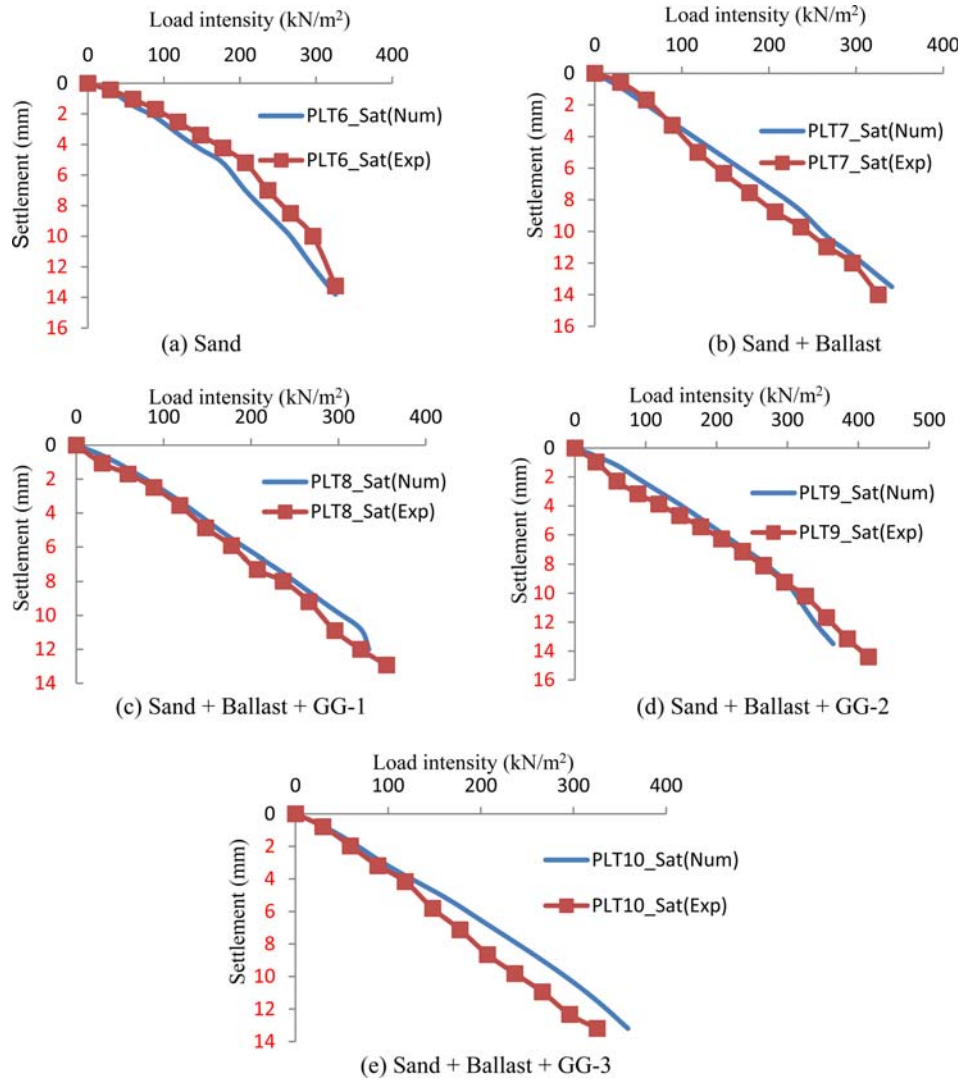


Fig. 16 Validation for square footing of 150 × 150 mm on sand, ballast and different geogrid in box of 500 × 500 × 400 mm under static load in wet condition

Table 9 Comparison of load intensity and settlement of different conditions of static load tests

Material details	Load intensity (kN/m <sup>2</sup> )	Settlement (mm)
Sand (Dry)	355	11.8
Sand + Ballast (Dry)	355	13
Sand + Ballast + Geogrid (GG-1) (Dry)	384.6	11.43
Sand + Ballast + Geogrid (GG-2) (Dry)	355	12.18
Sand (Wet)	325	13.25
Sand + Ballast (Wet)	325.5	14
Sand + Ballast + Geogrid (GG-1) (Wet)	384.5	12.9
Sand + Ballast + Geogrid (GG-2) (Wet)	325	13.19

With the inclusion of geosynthetics the  $C_u$  value increases. Thus with the same foundation area if geosynthetic is used, the subgrade modulus is increased and hence higher speed train can be used in such tracks.

The stiffness of the foundation-reinforced-soil system can be determined by using following equations

$$K_z = C_u A \text{ and } K_x = C_\tau A \quad (6)$$

The natural frequency of the foundation-reinforced-soil system is calculated using the following equation

$$\omega_n = (k/m)^{1/2} \quad (7)$$

where  $m$  is the mass of the machine plus foundation block. The spring constant  $k$  is the force required for unit displacement. For vertical vibrations, the spring constant  $k$  is taken to be proportional to the coefficient of elastic uniform settlement. After knowing the frequency of the vibration for a machine one can design the machine foundation using the natural frequency of the foundation-reinforced-soil system.

### 5.2 Effect of geogrid in machine foundation design

For design of machine foundation on reinforced sand for various reinforcing conditions one can follow the design steps as below

For unreinforced soil say sand and ballast in dry condition  $C_u$  value was  $2.28 \times 10^4$  kN/m<sup>3</sup> and that with geogrid (GG-1) it was  $3.39 \times 10^4$  kN/m<sup>3</sup>. Now using Eq. (4) we can find out the percentage decrease in area when geogrid is used as reinforcement

$$C_u \sqrt{A} = C_{u1} \sqrt{A_1}$$

Here,  $C_u = 2.28 \times 10^4$  kN/m<sup>3</sup> and  $A = 0.15 \text{ m} \times 0.15 \text{ m} = 0.0225 \text{ m}^2$ ,

For a value of  $C_{u1} = 3.39 \times 10^4$  kN/m<sup>3</sup>, the foundation area  $A_1$  works out as  $0.0101 \text{ m}^2$  which is 60% less than that for unreinforced case. Thus it has reduced the foundation area from  $0.15 \text{ m} \times 0.15 \text{ m}$  to  $0.1 \text{ m} \times 0.1 \text{ m}$ .

Difference in area =  $A - A_1 = 0.0153 \text{ m}^2$

### 5.3 Effect of geogrid in CBR value

$C_u$  is defined as the ratio of uniform pressure imposed on the soil to the elastic part of the settlement ( $S_e$ ). Thus

$$C_u = p/S_e \text{ (kN/m}^3\text{)} = \frac{(p)\text{from CBR}}{\text{Elastic settlement}} \quad (8)$$

where  $p$  is the bearing pressure (load per unit area, kN/m<sup>2</sup>) from the CBR.  $C_u$  is related to the soil and plunger parameter.

Now, to see the effect of geogrid in CBR value, let us consider value of  $C_u$  for unreinforced soil as  $C_u = 2.28 \times 10^4$  kN/m<sup>3</sup> and for reinforced soil  $C_{u1} = 3.39 \times 10^4$  kN/m<sup>3</sup>,

From Eq. (8),  $[p]_{CBR} = C_u \times \text{Elastic settlement } (S_e)$

Assuming the elastic settlement as 10% of the plate width,

Table 10 Computed CBR values for two different cases

Unreinforced case	Reinforced case
$[p]_{CBR} = C_u \times (0.1 \times 0.15) = 312 \text{ kN/m}^2$	$[p]_{CBR_1} = C_{u1} \times (0.1 \times 0.15) = 508 \text{ kN/m}^2$
$P_t = 312 \times 0.15 \times 0.15 \text{ kN} = 7.02 \text{ kN}$	$p_{t_1} = 508 \times 0.15 \times 0.15 \text{ kN} = 11.44 \text{ kN}$
$P_s = 20.55 \text{ kN}$ corresponding to 5 mm penetration, hence CBR = 34%	$P_s = 20.55 \text{ kN}$ corresponding to 5 mm penetration, hence CBR <sub>1</sub> = 56%

The load ( $P_t$ ) value of the CBR is then determined as below

$$P_t = [p]_{CBR} \times \text{plate area} \quad (9)$$

Where plate area =  $0.15 \times 0.15 \text{ m}^2$

Now CBR can be computed as

$$CBR = (P_t/P_s) \times 100 \quad (10)$$

Where  $P_t$  = Corrected test load and  $P_s$  = Standard load. The results are summarized in Table 10.

## 6. Conclusions

1. The load carrying capacity increases by 8% to 20% when geosynthetic is placed in between the sand bed and the ballast depending upon the tensile strength of geosynthetic.

2. The coefficient of uniform elastic compression increases by 10% and more depending upon tensile strength of geogrid when the same is used in between sand and ballast layer. Therefore design of machine foundation can be more economical as lesser area of machine foundation shall be adequate to cater that load.

3. The values of elastic modulus from cyclic load test are used to determine stresses which can be used to design blanket thickness for roads. From the relationship between  $C_u$  (coefficient of uniform elastic compression) and elastic modulus ( $E$ ). The  $C_u$  can be computed for designing the blanket thickness or subgrade thickness for roads and also for railways.

4. As the value of  $C_u$  increases, the elastic modulus ( $E$ ) also gets increased. Hence, rail tracks, if stabilised by geogrid, may allow higher speed trains over them. Therefore it can be concluded that by using geogrid in ballasted track, the efficiency of the ballast increases and thus the performance of railway track will also improve.

## References

- American Railway Engineering Association AREA (1996), American Railway Engineering Association Manual AREA, USA.
- Barkan, D.D. (1962), "Dynamics of bases and foundations", McGraw-Hill, New York.
- Indraratna, B., Ionescu, D. and Christie, D. (1998), "Shear behaviour of railway ballast based on large-scale triaxial tests", *Geotech. and Geoenviron. Eng. - ASCE*, **124**(5), 439-439.
- Indraratna, B., Khabbaz, H., Salim, W. and Christie, D. (2003), "Geotechnical characteristics of railway ballast, and the role of geosynthetics in minimising ballast degradation and track deformation", *Proceedings of RAILTECH 2003, Railway Technology in the New Millennium*, Kuala Lumpur, pp. 3.1-3.22.

- IS 5249: 1992, “Determination of dynamic properties of soil – method of test (Second Revision)”, Bureau of Indian Standards.
- Kumar, A. and Awasthi, S.K. (2008), “New concept of two-layer blanket system for track formation for heavy axle load”, *Proc. IPWE Seminar*, Lucknow, India.
- Kumar, A. and Saxena, A.K. (2009), “Track formation for high speed and heavy axle load”, *International Technical Seminar of IPWE*
- Lokesh, B.V. (2005), “Study of behaviour of ballast using geosynthetics”, M. Tech project report, Dept. of Civil Eng., IIT Roorkee.
- Mittal, Satyendra & Shukla, J.P. (2009), “Soil testing for engineers”, Khanna Publishers, New Delhi, India.
- Ramesh, H.N., Manoj Krishna, K.V. and Mamatta, H.V. (2010), “Compaction and strength behaviour of lime-coir fiber treated black cotton soil”, *Geomech. and Eng.*, **2**(1), 19-28.

PL

## Notations

$D_{60}$	: Grain size corresponding to 60% finer
$CBR$	: California bearing ratio
$C_u$	: Coefficient of uniformity
$C_c$	: Coefficient of curvature
$C_u$	: Coefficient of elastic uniform
$C_\tau$	: Coefficient of elastic shear
$C_\phi$	: Coefficient of elastic non-uniform shear
$C_\psi$	: Coefficient of elastic non uniform compression
$E$	: Elastic modulus of soil
$e_{max}$	: Maximum void ratio
$e_{min}$	: Minimum void ratio
$IS$	: Indian standard
$P_t$	: Corrected test load
$P_s$	: Standard load
$S_e$	: Elastic rebound settlement corresponding to ‘ $p$ ’ in mm
$S_p$	: non-recoverable settlement
$\nu$	: Poisson’s ratio
$\Phi$	: Angle of internal friction